Current Trends in Energy and Sustainability 2017 Edition

Invited Editors: Roberto Gómez-Calvet (Univ. Europea de Valencia)
José M. Martínez-Duart (Univ. Autónoma de Madrid)

Symposium on Energy and Sustainability. XXXVI Biennial.
Spanish Royal Physics Society
Santiago de Compostela (Spain), July 17-21. 2017

Book title: Current Trends in Energy and Sustainability. 2017 Edition
Invited Editors: Roberto Gómez-Calvet (Universidad Europea de Valencia) and José M. Martínez-Duart (Universidad Autónoma de Madrid).
(roberto.gomezcalvet@universidadeuropea.es - martinez.duart2@gmail.com)

ISBN: 978-84-0903541-0
Depósito Legal: M-26519-2018

Hybrid Brayton thermosolar systems: thermodynamic prediction of annual efficiencies and emissions

R.P. Merchán[1,*], M.J. Santos[1], A. Medina[1], A. Calvo Hernández[1]

[1] Department of Applied Physics, University of Salamanca, Plaza de la Merced s/n, 37008, Salamanca, Spain

* rpmerchan@usal.es

1. Introduction

The necessity to diversify the energy sources in power generation and to look for renewable ones is undoubted. Thermosolar power plants, which constitute one of the main ways of solar energy exploitation, are competing with other renewable energy sources for generating clean electrical energy, reducing fuel consumption. Hybrid thermosolar plants combine two great advantages on electricity generation: the emissions reduction of thermosolar energy, as well as the stable supply of power output to the grid of conventional power plants, avoiding the use of storage systems. For those reasons in the last years a big effort has been done in the development of prototypes and experimental plants in order to investigate the viability of thermosolar hybrid Brayton cycle plants.

A working fluid, usually air, is preheated by concentration solar energy, before entering a combustion chamber. Then, the fluid performs a thermodynamic cycle (in this case, a Brayton cycle), generating electrical energy indirectly. In this way fossil fuel and the associated emissions are reduced. It is important to note that apart from being easily scalable, gas-turbines can be combined with other cycles like bottoming Rankine. Also they do not require too much water for operation, which makes them suitable for electrical generation in arid regions, and are extremely versatile [1].

Experimental projects and prototypes developed up to date show that this technology is viable, but they also reveal that it is necessary to improve their efficiency, in order to generate electricity at competitive prices. Apart from R+D projects, prototypes, and experimental installations, several research works have been published in the last times. Some of them make use of commercial simulation environments, which allow a detailed description of all plant components and specific calculations on the solar subsystem. However, it is not easy to extract direct physical information about the main losses sources in the plant and to perform a global optimization of the plant design. Because of this reason, in this paper the next modus operandi is followed instead of this one.

A second type of strategy is to build a theoretical model of the plant, in terms of a reduced number of parameters, allowing a simple but realistic picture of plant operation and to estimate its performance records. Thermodynamic analyses can provide an integrated point of view of all subsystems and their importance in the overall efficiency. Moreover, they help to predesign future generations of plants based in this concept because of their flexibility to survey the adequate intervals of key parameters for optimal plant operation.

There are several theoretical works that start from the ideal Brayton cycle and thereafter refinements are included in the analysis of the thermodynamics of the cycle in order to recover realistic output records. Usually, in these works, the model for the concentrated solar subsystem, although including the main heat transfer losses, is simple. This allows to obtain closed analytical expressions for thermal efficiencies and power output, and then check the model predictions for particular design point conditions, with fixed values of direct solar irradiance and ambient temperature. But also by means of this thermodynamic model, a dynamic analysis that varies solar irradiance and external temperature conditions with time can be carried out. And in a possible step forward to suggest and guide optimization strategies.

2. Plant thermodynamics

A thermodynamic model for hybrid Brayton thermosolar plants, which has been proposed recently by the same authors, is going to be presented [2-5]. These plants have three main elements: the heliostat field, the receiver, and the power conversion system. The model, in which refers to the thermodynamic cycle, starts from a closed Brayton cycle however incorporating the main losses and irreversibility sources: pressure decays, non-ideal compressor and turbine, heat transfer losses in the solar collector, combustion inefficiencies, heat exchangers, etc.

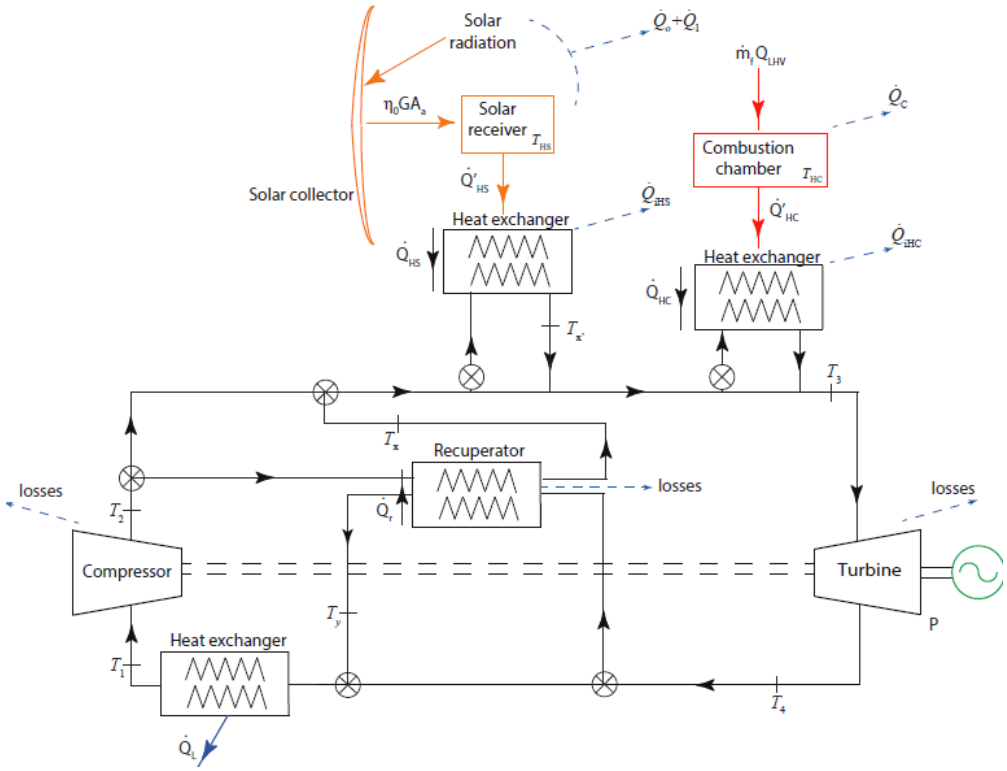

Figure 1. Scheme of the hybrid solar Brayton plant considered. The main heat transfers and temperatures are shown. Also the key losses sources considered in the model are depicted.

A central tower hybrid solar thermal installation, as depicted in Fig. 1, is considered. The whole system receives two energy inputs. On one hand, a heat input, GA_a, coming from the sun, where G is the direct solar irradiance and A_a, the aperture area of the solar field. For the solar subsystem, a simple model, which accounts for heat losses in the solar collector due to radiation and conduction/convection terms, was supposed.

$$\eta_S = \eta_0 - \frac{1}{GC}\left[\alpha\sigma(T_{HS}^4 - T_L^4) + U_L(T_{HS} - T_L)\right] \qquad (1)$$

In this equation η_S is the solar collector efficiency, η_0 the optical efficiency, C the concentration ratio, α the effective emissivity of the collector, σ the Stefan-Boltzmann constant, T_{HS} the collector working temperature, T_L the ambient temperature and U_L the conduction/convection heat loss coefficient.

On the other hand, the energy input at the combustion chamber is $\dot{m}_f Q_{LHV}$, being $\dot{m}_f$ the fuel mass flow rate and Q_{LHV}, its corresponding lower heating value. Finally, the heat engine generates a mechanical power output, P, and releases a heat flux to the ambient, $\dot{Q}_L$.

The overall thermal efficiency (η) was found as a function of the efficiency of the plant subsystems (solar η_S, combustion η_C, and gas turbine η_H), the effectivenesses of the heat exchangers linking subsystems (ε_{HS} for solar subsystem and ε_{HC} for combustion subsystem) and the solar share fraction (f).

$$\eta = \eta_S \eta_C \eta_H \left[\frac{\varepsilon_{HS}\varepsilon_{HC}}{\eta_C \varepsilon_{HC} f + \eta_S \varepsilon_{HS}(1-f)} \right] \qquad (2)$$

There is another interesting performance, denominated fuel conversion rate, that relates power output to the required heat with an associated economical cost (fuel burned). It does not represent a thermodynamic efficiency because it is defined in the range $[0, \infty]$:

$$\eta_e = \frac{P}{\dot{m}_f Q_{LHV}} = \frac{\eta \eta_S \eta_H \varepsilon_{HS}}{\eta_S \eta_H \varepsilon_{HS} - \eta f} \qquad (3)$$

A mass rate of an ideal gas (pressurized air) undergoes an irreversible recuperative closed Brayton cycle, in which the recuperator can be removed. The working gas is first compressed in a non-ideal compressor; and then it is heated up by the recuperator, the solar collector, and the combustion chamber. After the heating stage, the air is expanded and cooled irreversibly through a non-ideal turbine. And finally, the working gas recovers its initial conditions releasing heat with the recuperator and with another heat exchanger that connects the cycle to the surroundings. Turbine model includes these existing losses and irreversibilities. On the one hand, the geometric parameters related to the size of the cycle are taken into account. And, on the other hand, the heat losses irreversibilities in the compressor and turbine, in the recuperator and in all the heat exchangers and the pressure drop irreversibilities in the heat absorption and extraction processes are included. The key of the model resides in the fact that all the involved temperatures can be expressed in terms of the whole set of geometric and irreversibility parameters, so the performance of the plant is a function of these parameters [2].

3. Numerical implementation and validation

Once the thermodynamic model has been proposed, a numerical implementation is performed. This validation has been widely addressed by the same authors in [2].

Table 1. Top: output records from the manufacturer and from our model for the pure combustion mode. Bottom: estimated parameters and efficiencies from our model for the hybrid thermosolar mode.

GAS TURBINE: PURE COMBUSTION MODE			
Mercury 50 turbine: manufacturer's output records (*Caterpillar*)			
$T_3 = 1423\ K$	$T_y = 647\ K$	$\eta_h = 0.385$	$\lvert\dot{W}\rvert = 4.6\ MW$
Model: estimated output records			
$T_3 = 1418\ K$	$T_y = 650\ K$	$\eta_h = 0.387$	$\lvert\dot{W}\rvert = 4.5\ MW$
Relative deviations			
0.4 %	0.4 %	0.6 %	1.4 %
GAS TURBINE: HYBRID THERMOSOLAR MODE (at design point)			
Estimated output parameters			
$T_3 = 1423\ K$	$f = 0.42$	$\dot{m}_f = 0.151\ kg/s$	$\lvert\dot{W}\rvert = 4.2\ MW$
Estimated efficiencies			
$\eta_H = 0.393$	$\eta_S = 0.697$	$\eta = 0.317$	$\eta_e = 0.647$

In order to introduce the solar heat, researchers from SOLUGAS Project [6] have modified *Mercury 50* turbine (manufactured by *Caterpillar*). Output values of our model can be obtained and compared to the ones of manufacturer for the pure combustion mode (see Table 1). In accordance with this, relative deviations are very small, hence the turbine model agrees very well with real turbine data.

However, it is not possible to validate the thermosolar plant itself because the owner company has not published all the results, but a stationary estimation at the design point can be done. In this way, output parameters and efficiencies are estimated and all the results are perfectly reasonable, so it is concluded that the thermosolar plant model works fairly properly.

4. Results

4. 1. Temperature dependent specific heat (c_p)

Needed meteorological data (solar direct irradiance and ambient temperature) have been obtained from *Meteosevilla* database [7]. As probably Solugas design point conditions are too optimistic, average conditions are taken into account. So, an average calculation process is followed for obtaining annual mean values of these meteorological data [4]. In this way, the surrounding averaged temperature is $T_L = 291.575\ K$, while annual mean solar irradiance is $G = 457.874\ W/m^2$. This last one value can be considered a realistic value since it constitutes about half of the design point irradiance considered in Solugas project, $G = 860\ W/m^2$ [6].

As the temperature changes in this Brayton cycle are high (from about $300K$ to approximately $1400K$), the influence of the temperature on the specific heat, $c_p(T)$, may be important. The polynomial fit for this constant pressure specific heat has been determined by taking into account NIST data through RefProp software [8]. In order to analyze this influence, a comparison between the case when specific heat is supposed constant and the case when specific heat depends on the temperature has been carried out.

Table 2 shows these results together with relative deviations between the two alternatives, related to the temperature dependent case:

$$\Delta x\ (\%) = \frac{x_{c_{p(T)}} - x_{\bar{c}_p}}{x_{c_{p(T)}}} * 100 \qquad (4)$$

Table 2. Comparison of output values for temperature independent ($\bar{c}_p$) and dependent specific heat ($c_p(T)$), with relative deviations (Δx (%)).

WITH RECUPERATION	AVERAGE CONDITIONS		
	$\bar{c}_p$	$c_p(T)$	Δx (%)
η	0.323	0.324	0.475
η_e	0.449	0.450	0.267
η_S	0.610	0.609	−0.472
η_H	0.392	0.393	0.463
f	0.163	0.161	−1.023
$T_{HS}\ (K)$	948.886	971.150	2.293
$P\ (MW)$	4.621	4.677	1.207
$m_{f,spec}\ (kg/MWh)$	170.037	169.582	−0.268

In view of the results the differences between output variables with $\bar{c}_p$ and $c_p(T)$ are very small. For instance, overall thermal efficiency, solar collector efficiency, and solar share change only in the third decimal place. At the other extreme, temperatures present larger changes, although they are still small.

The main conclusion obtained from this study is that both models can be applied because results are very similar. So henceforth the model with constant specific heat will be used, since it is simpler and allows a completely analytical description. But the opposite approach, the cycle with temperature dependent specific heat, has been followed in [5]. It should be highlighted that our result contradicts conclusions from [9].

4. 2. Theoretical limits of the plant

Starting from real conditions (also called operating point), other four hypothetical configurations can be investigated with the goal of examining possible plant improvements over the real conditions of the plant: first the heat exchangers are considered as ideal, then the solar subsystem, after it is the Brayton cycle which is supposed ideal, and finally a completely ideal system is assumed. (see Fig. 2).

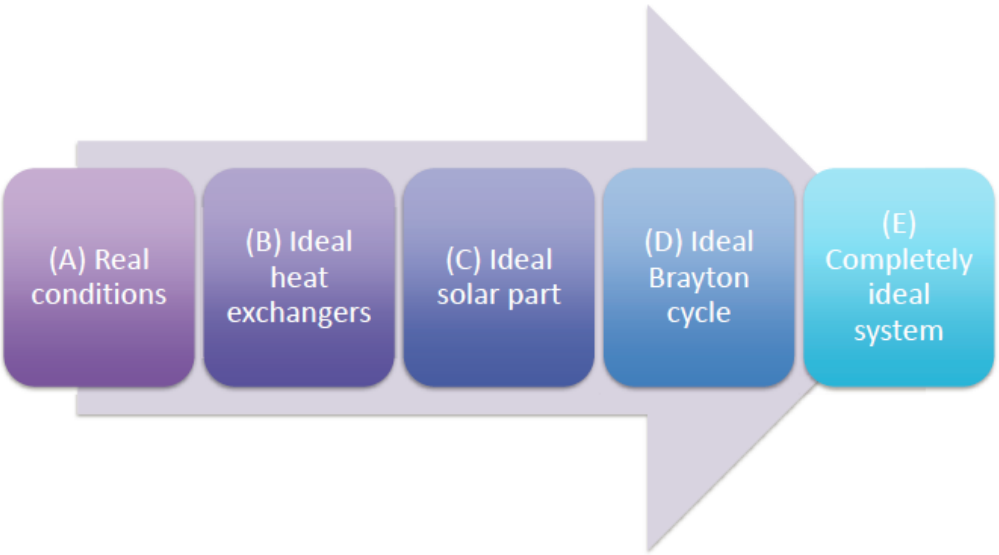

Figure 2. Scheme of the analyzed cases.

Apart from those five configurations, four operating modes are analyzed according to the existence or not existence of solar input and recuperator.

At real conditions (Table 3), a power output of 4.5 MW can be achieved, very close to that of the design point. It should be highlighted that exhaust temperature presents a high value in all cases, which is important to take advantage of residual heat with cogeneration or bottoming cycles.

Overall thermal efficiency of the recuperative plant is larger if there is no solar input: a 6.9 % higher than for hybrid operation, due to energy losses in solar subsystem associated with high temperatures. On the other hand, fuel conversion rate takes its larger value when there is solar input and recuperation. It can be confirmed that, in combustion mode, the fuel conversion rate is the overall thermal efficiency. In addition, solar collector efficiency is relatively good; however, solar share is still small.

Table 3. Annual means of most important plant performance records: (A) operating point. Relative differences are calculated with respect to the layout with no solar input.

Operating point (A)	Without recuperation		With recuperation	
	Without solar input	With solar input	Without solar input	With solar input
$P\ (MW)$	4.370	4.377 (+0.16%)	4.469	4.476 (+0.16%)
η	0.262	0.250 (−4.75%)	0.367	0.342 (−6.94%)
η_e	0.263	0.283 (+7.39%)	0.367	0.406 (+9.54%)
η_H	0.274	0.274 (+0.04%)	0.383	0.383 (+0.08%)
$T_{HS}\ (K)$	–	730.1	–	946.6
η_S	–	0.620	–	0.586
f	–	0.123	–	0.164

Table 4 is obtained when a completely ideal system is assumed. So, these are the maximum achievable values that mark the plant performance limits. A great power output can be reached: almost $8\ MW$. Also, an overall efficiency of 0.6, a fuel conversion rate of about 0.8, and a solar share of 0.3 (double that for the real conditions) are predicted.

Table 4. Annual means of most important plant performance records: (E) completely ideal system. Relative differences are calculated with respect to the layout with no solar input.

Completely ideal system (E)	Without recuperation		With recuperation	
	Without solar input	With solar input	Without solar input	With solar input
$P\ (MW)$	7.988	7.988 (+0.%)	7.988	7.988 (+0.%)
η	0.452	0.452 (+0.%)	0.628	0.628 (+0.%)
η_e	0.452	0.522 (+15.68%)	0.628	0.792 (+26.0%)
η_H	0.452	0.452 (+0.%)	0.628	0.628 (+0.%)
$T_{HS}\ (K)$	–	722.1	–	971.0
η_S	–	1.	–	1.
f	–	0.218	–	0.301

The intermediate configurations have been also analyzed [4], but for the sake of brevity their tables results are not exposed here. As a summary, Fig. 3 is presented, where some output records are shown for the five configurations. It is clear that configurations (D) and (E), that is to say, assuming the Brayton cycle and the whole system as ideal, is which affects more to overall efficiency, to fuel conversion rate and to power output.

When the solar subsystem is supposed ideal, the solar collector efficiency raises fairly significantly. However, these increments are not reflected on the overall thermal efficiency.

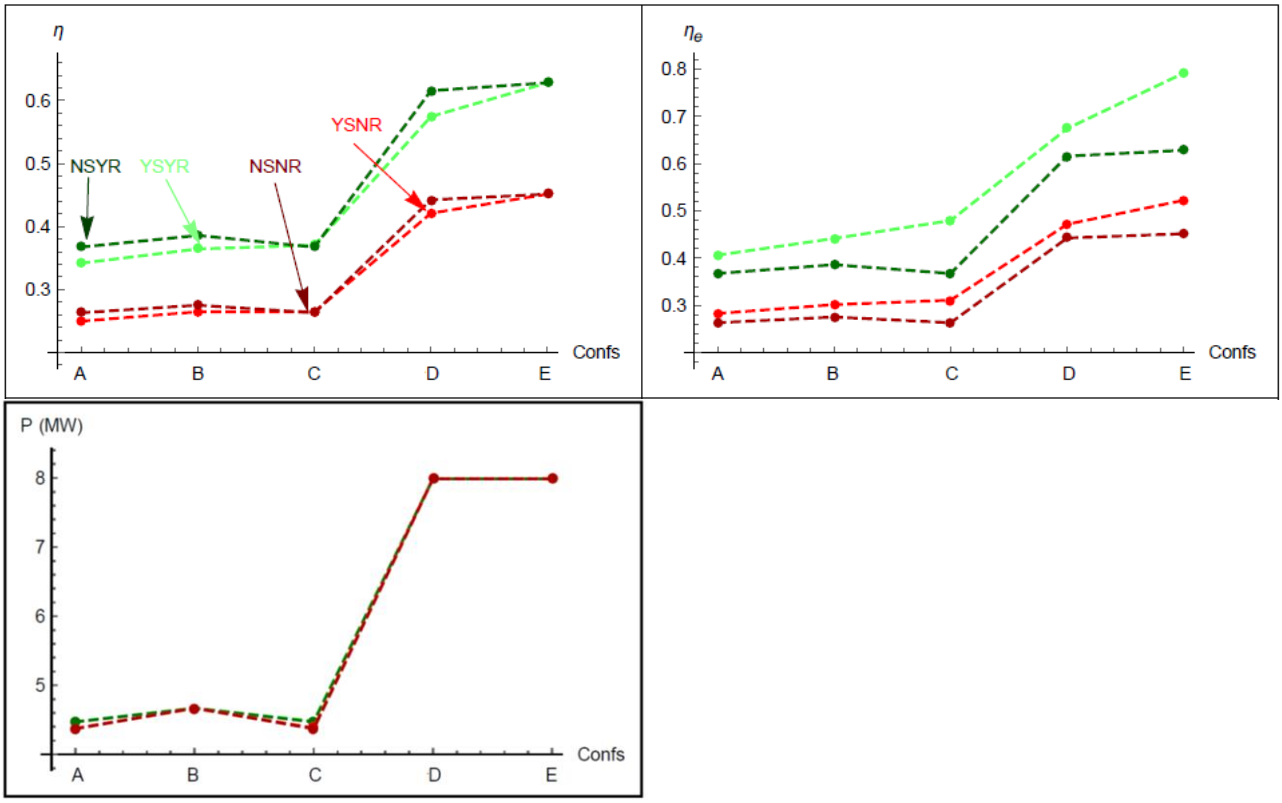

Figure 3. Some output records for the five layouts. Top left: overall thermal efficiency, η; up right: fuel conversion rate, η_e; bottom left: power output, P. The lines between dots are just a guide for the eyes. Legend: YSYR= With solar input and with recuperation, NSYR=Without solar input and with recuperation, YSNR=With solar input and without recuperation, NSNR=Without solar input and without recuperation.

In Figs. 4 and 5 two Sankey diagrams representing the main plant losses can be seen for the real conditions configuration as well as for the layout when the completely system is assumed as ideal. Looking at the solar part, $\dot{Q}_l$ and $\dot{Q}_{iHS}$ are the losses associated to the heat transfers on the solar receiver and $\dot{Q}_{HS}$ denotes the heat rate input from the solar collector. And regarding at combustion part, $\dot{Q}_C$ is related to the heat losses in combustion subsystem, $\dot{Q}_{iHC}$ refers to the heat losses at its heat exchanger and $\dot{Q}_{HC}$ is the heat rate input from combustion chamber.

These energy fluxes are normalised to unity and so, in the first case, the solar input is 26 % of the total and the combustion input constitutes the rest, 74 %. It is quite visible that the first diagram presents small energy losses both in combustion and solar subsystems; while the other does not have any heat loss.

Moreover, it must be stressed that, at real conditions, the wasted heat flux, which is released to the ambient, is higher than the one of power output; however, in the completely ideal system configuration, the power output flux is quite higher than the wasted heat, due to the high increment of heat engine efficiency. Despite Brayton cycle subsystem can achieve the highest improvements for the performance of the hybrid plant, technical feasibility and room for improvement have to be considered, since it may be easier to improve solar subsystem performance, due to the fact that thermosolar technology is considerably less mature than gas-turbine equipment.

On the other hand, the solar flux is always smaller than the combustion one, since the solar share does not exceed 30 % in any case. This fact means that the solar collector field is very small for the desired power output, and so the turbine inlet temperature required for obtaining this power is not reached only with solar subsystem. Therefore it is always necessary to burn quite fuel. This is a plant sizing problem, which is solved by reducing the power output supplied to the grid or by increasing the heliostat field size.

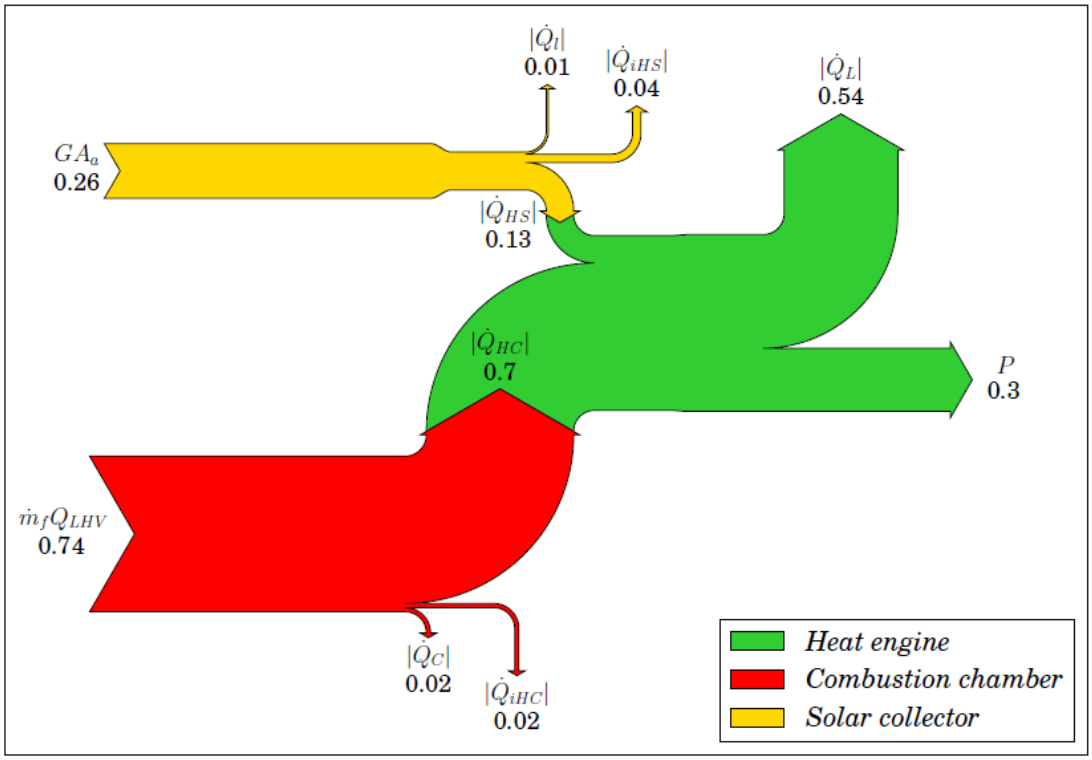

Figure 4. Sankey diagram for the real conditions configuration (A), for the hybrid recuperative case. Energy fluxes are normalised to unity.

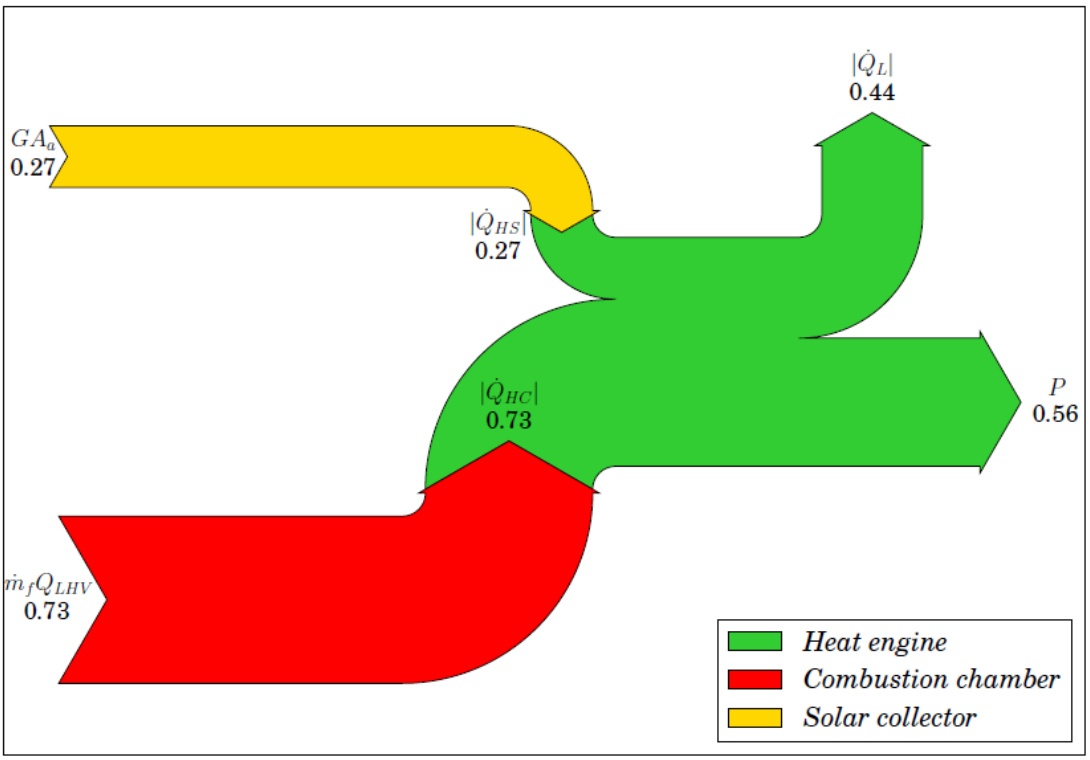

Figure 5. Sankey diagram for the completely ideal system (E), for the hybrid recuperative case. Energy fluxes are normalised to unity.

Finally, the specific natural gas consumption and the pollutant emissions can be analyzed. They are directly estimated through the natural gas emission factors. However, the calculated predictions on emissions should only be taken as a guide, because each plant could have particular technologies to reduce emissions or CO_2 capture mechanisms.

In Table 5 both specific fuel consumption and emissions are collected for the operating point case (A). In the case of recuperation and solar input, the fuel consumption is about 187 kg/MWh, value that rises until 284 kg/MWh when no recuperation and no solar input are taken. Comparing pure combustion and hybrid modes, fuel savings of 8.3 % and 6.2 % can be achieved for recuperative and non-recuperative cases, respectively. These percentages can seem relatively small, but this consumption saving can supposed important advantages for companies in annual terms.

Table 5. Annual means of fuel specific consumption and of specific emissions: (A) real conditions.

Operating point (A)	Without recuperation		With recuperation	
	Without solar input	With solar input	Without solar input	With solar input
$m_f\ (kg/MWh)$	283.995	266.463	203.485	186.569
$CO_2\ (kg/MWh)$	702.758	659.374	503.534	461.674
$CH_4\ (g/MWh)$	13.296	12.475	9.527	8.735
$N_2O\ (g/MWh)$	1.291	1.211	0.925	0.848
Relative differences	−6.173%		−8.313%	

Also, it is important to note that, comparing recuperative and non-recuperative modes, a 30 % of fuel reduction can be reached for solar input and a 28 % for no solar input.

In addition, the pollutant gases emission associated with the natural gas burning are estimated, namely, the methane, the nitrous oxide, and the carbon dioxide generation. Specific emissions of carbon dioxide at normal performance (operating point, recuperation, and solar input) are $CO_2 = 461.674\ kg/MWh$, whereas those of CH_4 and N_2O are $CH_4 = 8.735\ g/MWh$ and $N_2O = 0.848\ g/MWh$, respectively.

Table 6. Annual means of fuel specific consumption and of specific emissions in the five configurations, for the hybrid recuperative case. The increments are relative differences of the particular configuration with respect to configuration (A).

With recuperation and solar input	Operating point (A)	Ideal heat exchangers (B)	Ideal solar part (C)	Ideal Brayton cycle (D)	Completely ideal system (E)
$m_f\ (kg/MWh)$	186.569	173.516	169.781	112.204	101.019
$CO_2\ (kg/MWh)$	461.674	429.374	420.13	277.654	249.977
$CH_4\ (g/MWh)$	8.735	8.124	7.949	5.253	4.730
$N_2O\ (g/MWh)$	0.848	0.789	0.772	0.510	0.459
Relative differences	–	−6.996%	−8.998%	−39.859%	−45.854

The same variables but for the five before mentioned configurations are displayed in Table 6, where also relative differences are shown with respect to operating point. Also here it is observed that the leap occurs when approaching the ideal Brayton power unit, with almost a 40 % of decrease in fuel consumption and pollutant emissions. Ideal heat exchangers and ideal solar part models give a smaller reduction on consumption: approximately 7 % and 9 %, respectively. Of

course, the completely ideal system configuration presents the higher decrease, around 46 %. Those percentages correspond with theoretical limits for greenhouse emissions reduction. Therefore, the room for improvement is wide. If the complete system was ideal, specific carbon dioxide emission would be $CO_2 = 249.977\ kg/MWh$, which is a very promising result.

In doing the same as before, comparing the carbon dioxide production for the five configurations, Fig. 6 can be obtained, where it is clearly visible that considering the Brayton cycle or the complete system as ideal have a great effect on emissions reduction, reaching the same values of before, 40 % and 46 %, respectively.

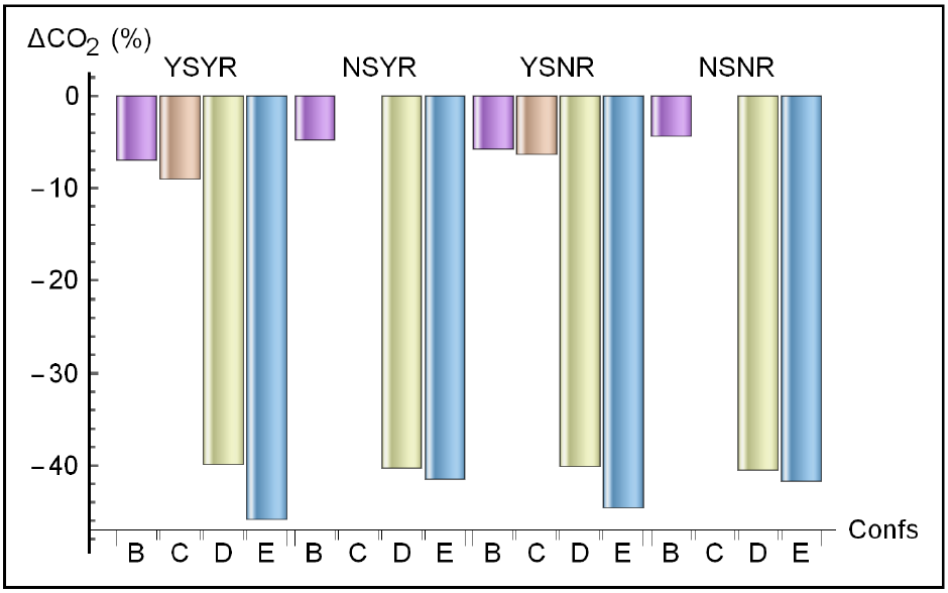

Figure 6. Relative differences of specific emissions of CO_2 between configurations (B)-(E) and configuration (A) quantified as relative increments in percentages with respect to the real conditions configuration (A). Hybrid and combustion modes and recuperative and non-recuperative configurations are considered. Legend: YSYR= With solar input and with recuperation, NSYR=Without solar input and with recuperation, YSNR=With solar input and without recuperation, NSNR=Without solar input and without recuperation.

4. 3. Sensitivity analysis

A sensitivity analysis is performed in order to study the influence of the main subsystems irreversibilities on the overall plant performance records. Heat engine losses parameters will be varied, starting from design point conditions. But also the influence of solar subsystem losses parameters and that of pressure losses in the heat absorption process, $\Delta p_H/p_H$, can be analysed [4].

Changes on the losses parameters associated to the heat engine will greatly affect plant performance, as it is surveyed in Fig. 7. The evolution of all variables is also almost linear, however the scales of the vertical axes indicate much more important variations on the performance records. For example, an increment of 10 % on compressor isentropic efficiency, ε_c, will lead to 10 % rise on power output and the same increment on turbine isentropic efficiency, ε_t, to more than 20 % on P. Great improvements are achieved when both the compressor and turbine efficiency are incremented simultaneously, almost 40 % on power output can be reached if $\varepsilon_c + \varepsilon_t$ rises up to 10 %.

As recuperation is an internal process of the heat engine, recuperator effectiveness changes would not have any influence on power output, nevertheless other output records would be affected. The other analyzed output records (overall efficiency, η, Brayton subsystem efficiency, η_H, and fuel conversion rate would, η_e) change in the interval $[-30\ \%, +30\ \%]$ for variations in the losses coefficients of the power unit in the interval $[-10\ \%, +10\ \%]$. In short, reductions on Brayton losses would be increased by a factor 3 on the plant records.

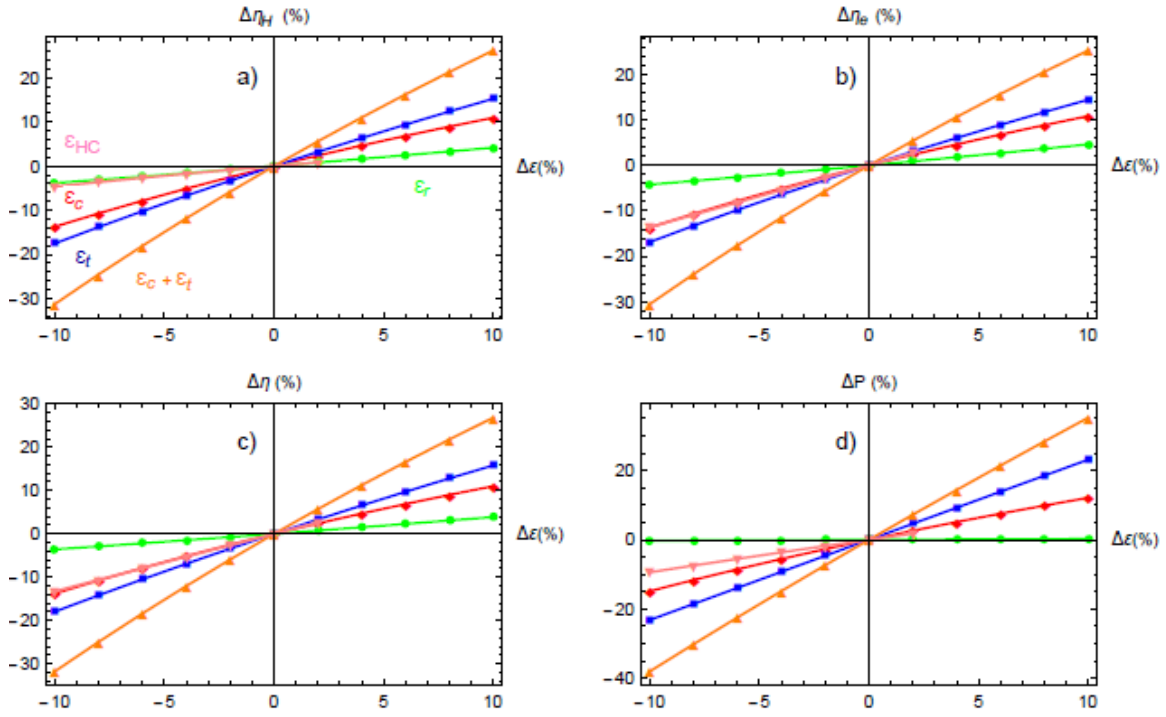

Figure 7. Sensitivity of different output records, power output (P), overall thermal efficiency (η), Brayton cycle efficiency (η_H), and fuel conversion efficiency (η_e), to several irreversibility parameters of the heat engine: isentropic efficiency of the turbine (ε_t), isentropic efficiency of the compressor (ε_c), recuperator effectiveness (ε_r), and effectiveness of the heat exchanger associated to the combustion chamber (ε_{HC}). Another case is also considered: when ε_c and ε_t are simultaneously changed in the same way. Both axis are represented in relative terms as percentages. The central point is related to the yearly averages of the recuperative plant at real operating conditions.

5. Future work

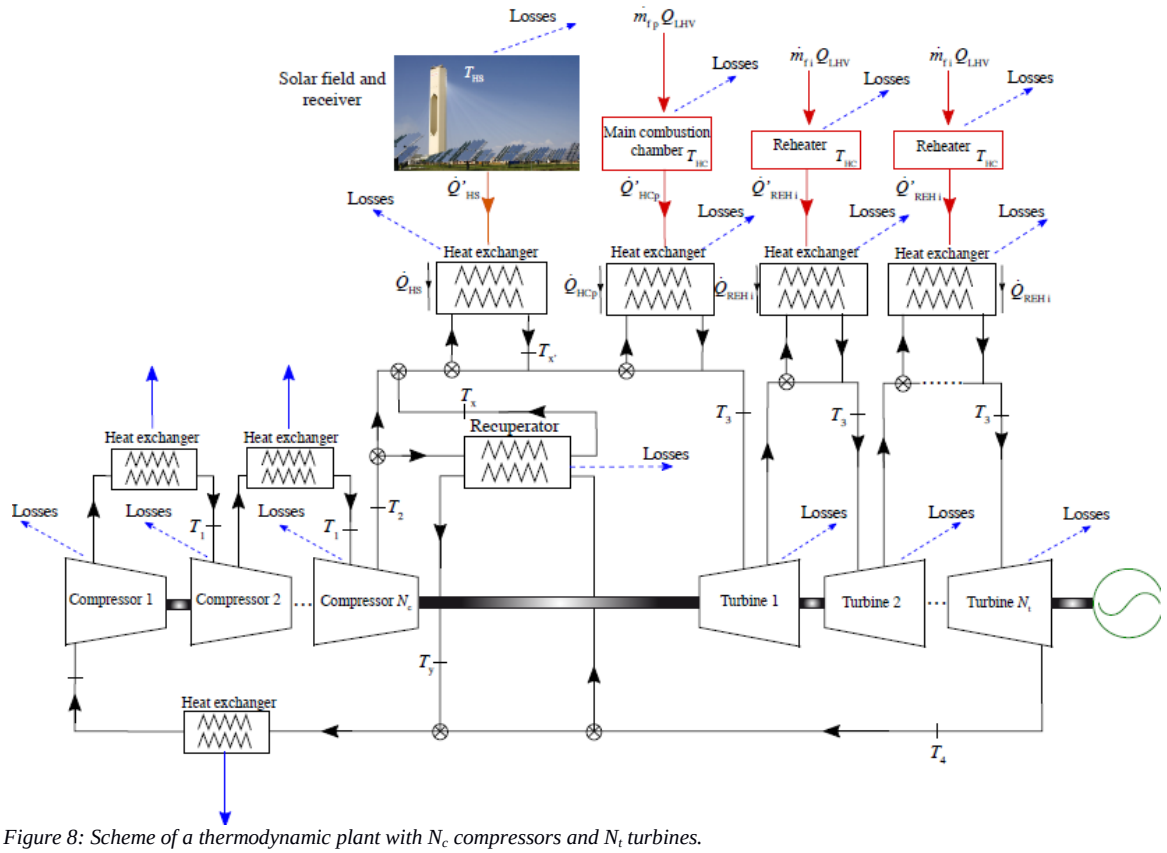

Figure 8: Scheme of a thermodynamic plant with N_c compressors and N_t turbines.

Currently this project continues with other lines of research, among them: multistage plants, different working fluids, parabolic dishes, and combined cycles.

The inclusion of several turbines and compressors in the thermodynamic plant's scheme (Fig. 8) results in an increase of the overall efficiency and of the net power, although the economic investment also rises.

Changing the working fluid from dry air to other less usual gases as nitrogen, helium or carbon dioxide can be beneficial from the viewpoint of the reduction of temperatures (CO_2) or the pressure losses (He), but it can also lead to some disadvantages like the lower experience (see Table 7) [10].

Table 7. Comparative table of some working fluids.

Working fluid	Advantages	Disadvantages
Dry air	Experience, abundant, free	High pressure losses, high temp.
N_2	Similar to air	High pressure losses, high temp.
He	Low pressure losses, inert, non-toxic	More stages, high temp., few experience, leaks
CO_2	Moderate temp., good critical point, inert, non-toxic	Fast variations of critical point, scarce experience

Another possibility for future work is to change the tower Central Receiver System by parabolic dishes, which allow an electric generation in a smaller scale, with only a few kW, thanks to the microturbines set up in their receivers. Therefore, parabolic dishes can be employed for distributed generation in isolated places without access to the electric gird or also, when lot of them are placed in fields, for releasing energy to the grid.

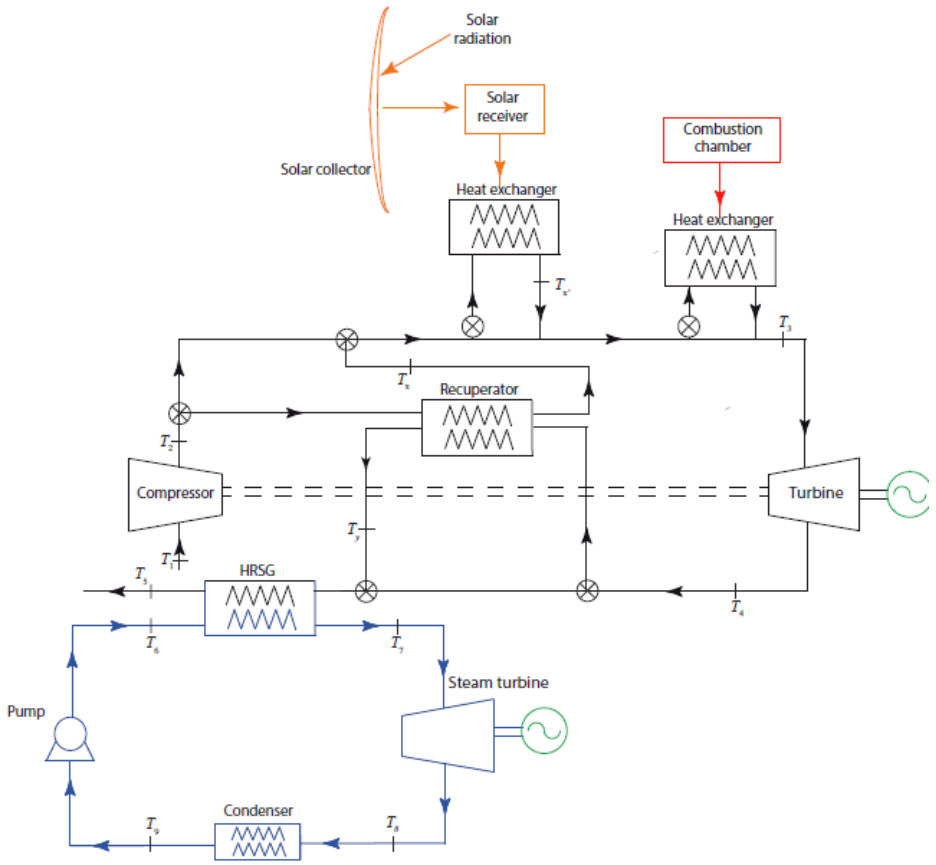

Figure 9: Scheme of a combined thermodynamic plant (Brayton cycle + Rankine bottoming cycle).

On the other hand, setting up a Rankine cycle bottoming the Brayton one (combined cycle) can lead to the use of the excess of heat after the turbine (Fig. 9) and can improve the overall efficiency and increase the power output.

6. Conclusions

Finally, the most important conclusions obtained from this study are summed up here:

- A thermodynamic model for a hybrid system composed of a solar central receiver heliostat field and a Brayton gas turbine was developed.
- Additionally, the system is described in terms of a reduced number of parameters, with clear physical meaning each.
- Furthermore, the model was validated by the consideration of the SOLUGAS Project, developed by the company Abengoa Solar, near Seville.
- Likewise, the model incorporates the main losses and irreversibility sources: non-ideality turbine and compressor, pressure decays, real heat exchangers, heat transfer losses in the solar collector, combustion inefficiencies, etc.
- It was shown that since the model is flexible, it allows to check the performance of several plant configurations.
- As summary, it can be said that the most important improvements are related to the Brayton cycle, since higher increments can be observed in all the variables.
- Also, it is interesting to stress that high increments on solar collector efficiency do not raise significantly overall thermal efficiency. Nevertheless, they can increase fuel conversion rate.
- As mentioned before, numerically, the most influential factor corresponds to improvements on Brayton cycle. On the other side, the technical possibilities have to be taken into account. This issue is outside the range of this study. However, we are aware that it has to be accounted, since Brayton cycle improvements may not be feasible nowadays, although they are the most effective ones, and perhaps the solar efficiency improvements are easier achievable.
- In conclusion, this kind of plants are especially interesting for regions with good insolation ratios and scarce hydric resources, because allow an appreciable reduction of fossil fuel consumption. There is still room for improvement in the economic issues, so further research and development are needed; but these facilities are worth the effort from the ecological point of view, since they reduce significantly pollutant emissions related to greenhouse effect, so they can help to mitigate the anthropogenic intensification of climate change.

Acknowledgments

The authors acknowledge financial support from MINECO of Spain, Grant ENE2013-40644-R and University of Salamanca.

References

[1] O. Behar, A. Khellaf, K. Mohammedi, *Rene. Sust. Energ.* **23** (2013) 12-39.
[2] D. Olivenza-León, A. Medina, A. Calvo Hernández, *Energ. Conv. Manage.* **93** (2015) 435-447.
[3] M.J. Santos, R.P. Merchán, A. Medina, A. Calvo Hernández, *Energ. Convers. Manage.* **115** (2016) 89-102.
[4] R.P. Merchán, M.J. Santos, I. Reyes-Ramírez, A. Medina, A. Calvo Hernández, *Energ. Convers. Manage.* **134** (2017) 314-326.
[5] R.P. Merchán, M.J. Santos, A. Medina, A. Calvo Hernández, *Renew. Energ.* xxx (2017) 1-11. https://doi.org/10.1016/j.renene.2017.05.081

[6] R. Korzynietz, J.A. Brioso, A. del Río, M. Quero, M. Gallas, R. Uhlig, M. Ebert, R. Buck, D. Teraji, *Sol. Energy* **135** (2016) 578-589.
[7] Meteosevilla. http://www.meteosevilla.com.
[8] E. W. Lemmon, M. L. Huber, M. O. McLinden. NIST Standard Reference Database 23: Reference fluid thermodynamic and transport properties-REFPROP, version 9.1. National Institute of Standards and Technology, Standard Reference Data Program, Gaithersburg (2013).
[9] L. Wu, G. Lin, J. Chen, *Renew. Energ.* **35** (2010) 95-100.
[10] O. Olumayegun, M. Wang, G. Kelsall, *Fuel* **180** (2016) 694-717.